Considerations on the Preliminary Sizing of Electrical Machines with Hairpin Windings

Mohammad Soltani
Dept. of Engineering Enzo Ferrari
University of Modena and Reggio Emilia,
Alma mater Studiorum University of Bologna
Modena, Italy
mohammad.soltani@unimore.it

Stefano Nuzzo
Dept. of Engineering Enzo Ferrari
University of Modena and Reggio Emilia
Modena, Italy
stefano.nuzzo@unimore.it

Davide Barater
Dept. of Engineering Enzo Ferrari
University of Modena and Reggio Emilia
Modena, Italy
dbarater@unimore.it

Giovanni Franceschini
Dept. of Engineering Enzo Ferrari
University of Modena and Reggio Emilia
Modena, Italy
giovanni.franceschini@unimore.it

***Abstract*— Although the standard preliminary sizing of electrical machines equipping random windings is well consolidated and is worldwide acknowledged to be a good starting point for the design, there is no proof of accuracy and confidence when it comes to hairpin windings. This winding technology is gaining extensive attention due to its inherently high slot fill factor, good heat dissipation, strong rigidity, and short end-windings. These features make hairpin windings a potential candidate for some traction application to enhance power and/or torque densities. In this paper, a comparative design is done using the classical sizing tools available in the literature between two surface-mounted permanent magnet synchronous machines, one featuring a random winding and one with a hairpin layout. The study aims at highlighting the hairpin winding challenges at high frequency operations and at showing limits of applicability of these standard approaches when applied to this technology. For verification purposes, finite element evaluations are also performed.**

Keywords—Hairpin windings, hairpin design, machine design, sizing

I. INTRODUCTION

Widespread research in the area of electric machines for traction applications is pushing the boundaries for high speed and power density with innovations in cores, magnets and winding designs [1]. These innovations also seek higher efficiency and lower costs. However, while higher speeds mean higher power for a given torque [2], they also result in additional losses in cores and windings thus lowering the overall efficiency, and in structural challenges relative to the rotating components. Hence, the design of an electric machine compliant with all the objectives mentioned above is a very complex task.

Permanent magnet (PM) motors are the most popular candidates for electric machines in traction applications [3]. Among these, interior PM (IPM) machines provide high power density, high efficiency and wide speed range, that are all required for traction applications. The stator winding of PM traction machines can be wound randomly, using stranded wires, or with form-wound windings made of flat bar conductors with a rectangular cross-section [4]. Form-wound windings are gaining popularity in traction applications. The most evident benefit of bar-wound windings over random-wound ones is the increased slot fill factor, i.e. the ratio between conductive and insulation materials inside the slot. In fact, random windings are made of wires with a circular cross-section, which will never match the slot shape, whatever it is. Contrarily, the flat rectangular wires can perfectly fit the shape of the slot when this is also rectangular, i.e. the slot features parallel sides along the radial machine direction. To strengthen this concept, in Figure 1a) and b), the "layered" round wire winding methods are illustrated, whereas Figure 1 c) shows a rectangular wire winding layout [5].

Of all the bar-wound windings, the hairpin type is rather wide-spreading. Here, a flat rectangular copper wire is preformed into a "hairpin" shape and inserted into the slot, and then the open sides are suitably twisted and welded to form a coil. In comparison with round windings, the end-winding length is thus shortened and, consequently, the DC copper loss is reduced [6]. Besides this end winding feature, the flat and "massive" shape of each hairpin leg reduces the DC copper loss produced by the active parts compared to their round-wound counterpart. Besides, in a series-production context, the hairpin windings manufacturing can be advantageous in terms of costs and cycle times in comparison with the traditional, often manual, random winding method [7]. For all these reasons, in traction applications, hairpin technologies are gaining more and more attention due to their potential in achieving higher power and torque densities [8-11]. However, this technology presents some drawbacks too. One of the major open points is the power loss at high frequency operations, which poses a limit on the applicability of machines with hairpin windings for high-speed applications. Many methods have already been proposed to overcome such

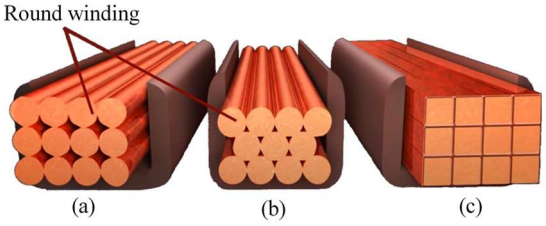

Figure 1 Qualitative view of a slot cross section for (a) regular round winding, (b) modified round winding, (c) rectangular winding

major challenge, [2], [12-15] and this is where the on-going research is focusing.

On the other hand, only a few works deal with a comparison in terms of design procedure between random and hairpin windings [16-17]. Therefore, in this paper, the aim is to use the classical sizing equations typically used for random-wound electric machines also for the preliminary design of machines equipping hairpin windings. As a case study, a surface mounted PM motor intended for a traction application is considered and a comprehensive comparison between random and hairpin winding designs is provided. Finite element (FE) evaluations are also performed for validation purposes, finally highlighting the limits of applicability of the classical sizing equations to the design of electrical machines with hairpin windings.

II. Preliminary Design process

A. Starting requirements and assumptions

The design process is initialized by defining some basic machine performance requirements, such as output power, speed, voltage and desired efficiency. The values of such input parameters are listed in Table I.

The second step is that of making some assumptions on the materials and the cooling system. M330-50A and NdFeB are used for cores and PMs respectively, whereas natural convection is hypothesized as a heat extraction method. This permits defining magnetic and electric loadings and the maximum flux density values allowed in the various parts of the motor. Some additional choices on the outer rotor diameter to axial length ratio, airgap thickness, PMs' span, number of slots-per-pole-per-phase and number of poles are initially made. The choice of the expected speed and the pole number is based upon the desired operating frequency chosen for the design exercise, i.e., 200 Hz. For a fully fair comparison between round and hairpin windings, the same number of slots-per-pole-per-phase, i.e. q=3, is assumed and the stator structure is based on a distributed full-pitch, single-layer winding. Given the low degrees of freedom allowed by hairpin windings, the number of conductors per slot z_q in both random and hairpin winding designs is set to 4. A summary of all these parameters is provided in Table II.

Considering the above and assuming the number of phases $m=3$, the slots number is calculated as $Q=q \cdot m \cdot 2p=72$ and the number of winding turns per phase as $N= z_q \cdot q \cdot p=48$. Also, given the type of winding structure initially assumed, the short pitch factor k_{cp} is equal to 1, while the distribution factor k_d is calculated as (1), where β is the slot pitch angle. The total winding factor k_w is given by the product of $k_{cp} \cdot k_d$.

It must be mentioned that some of the design parameters which were considered here as input design choices could be envisioned as output variables to be refined according to design requirements and constraints. However, for the sake of this paper, the described design process is reasonable.

B. Sizing calculations

Having preliminarily selected the D/L ratio, the starting point for the motor sizing, either with random or hairpin windings, is the torque expression given in (2). In (2) B is the RMS value of the fundamental airgap flux density B_{max} obtained from (3) using the Fourier series decomposition of a square wave waveform. Equation (2) permits finding the values of D and L. Then, hypothesizing in the PMs the same flux density as in the airgap, (4) can be used to determine the thickness l_m of the PMs.

Table I EXPECTED PERFORMANCE FROM PROTOTYPE DESIGN

Parameter	Symbol	Amount
Output power	P	37.7 kW
Speed	n_m	3000 rpm
Voltage	V_{LL}	370 V
Efficiency	η	95 %

Table II INITIAL DESIGN ASSUMPTIONS AND CHOICES

Parameter	Symbol	Amount
Linear current density	A	40 kA/m
Current density	J	5 A/mm^2
Airgap flux density	B_{ag}	0.8 T
Teeth flux density	B_t	1.6 T
Yoke flux density	B_y	1.4 T
Residual flux density of PMs	B_r	1.05 T
Relative permeability of PMs	μ_m	1.05
Outer rotor diameter / axial length	D / L	1.1
Air-gap thickness	g	1 mm
Pole number	2p	8
Pole span	α_{PM}	33°
Number of slots-per-pole-per-phase	q	3
Number of conductors per slot	z_q	4

The total area $S_{all\ slots}$ to be dedicated to the three machine phases can be calculated using (5), where k_{ff} is the slot fill factor. Yoke thickness W_y and tooth width W_t can be calculated using (6) and (7), respectively. In (6), Φ_p is the physical flux per pole, whereas in (7) λ_s is the stator slot pitch in meters.

It should be noticed that, so far, the sizing equations for both random and hairpin winding designs are basically the same. The only step where the hairpin design played a role was related to the decision of fixing the number of conductors per slot, which is usually derived from the rated voltage V_{ll} instead. However, the major difference in the calculations is dictated by the choice of the fill factor. While for round windings k_{ff} is relatively low and, thus, this is taken equal to 0.5, in hairpin windings the fill factor is higher and it is then assumed equal to 0.8 in this design exercise. These choices make the hairpin design inherently more compact than the round design, i.e. the outer stator diameter is smaller. Another important point of difference to mention is the slot shape. As recalled in Section I, a trapezoidal slot shape is envisioned for the machine with random windings, whereas a rectangular shape is considered for the machine with hairpin windings□

$$k_d = \frac{\sin(\frac{q.\beta}{2})}{q.\sin(\frac{\beta}{2})} \tag{1}$$

$$T = \frac{\pi}{2} D^2 L B A \tag{2}$$

$$B_{max} = \frac{4B_{ag}}{\pi}.\sin(\frac{p\,\alpha_{PM}}{180}.\frac{\pi}{2}) \tag{3}$$

$$l_m = \frac{\mu_r l_g}{\frac{B_r}{B_{ag}}-1} \tag{4}$$

$$A = \frac{J.S_{\text{all slots}}.k_{\text{ff}}}{\pi D} \tag{5}$$

$$W_y = \frac{\phi_p}{2B_y L} \quad (6)$$

$$W_t = \frac{B_{\text{avg}}.\lambda_s}{B_t} \quad (7)$$

C. Power losses

However, besides these design aspects, the most important factor to consider when designing an electrical machine with hairpin windings is the AC Joule losses. In random windings with stranded conductors, the AC losses can be neglected. Contrarily, in hairpin windings, AC losses need to be carefully considered and determined.

1) Copper loss: the DC resistance R_{DC} of a machine phase depends on the total length of one coil L_c, the number of turns in series N and parallel paths a per phase, the cross-sectional area of the conductor S_c and the conductivity of the conductor material σ_c [6]. Considering a uniform current distribution at any frequency in stranded conductors, the losses associated with the DC resistance is the only contribution in the random winding design. In hairpin conductors, the skin and proximity effects and the ensuing AC losses are usually determined through the ratio between R_{AC} and R_{DC}. For each layer k, this ratio (k_{Rk}) is determined using (8), where φ, ψ and ξ are expressed as in (9), (10) and (11), respectively. In (11), h_{c0} and b_{c0} are the height and width of the sub-conductors, respectively; ω is the supply frequency; μ_0 is the permeability of vacuum [18].

$$\square_{\text{Rk}} = \square(\square) + \square(\square - 1)\square(\square) \quad (8)$$

$$\square(\square) = \square \frac{\sinh 2\square + \sin 2\square}{\cosh 2\square - \cos 2\square} \quad (9)$$

$$\psi(\xi) = 2\xi \frac{\sinh \xi - \sin \xi}{\cosh \xi + \cos} \quad (10)$$

$$\xi = h_{c0}\sqrt{\frac{1}{2}\omega\mu_0\sigma_c \frac{b_c}{b}} \quad (11)$$

2) Iron loss: the laminations' manufacturers usually give the loss density in *W/kg,* at a specific frequency and flux density values. This includes both eddy current and hysteresis losses. Analytically, iron losses can be found by dividing the magnetic circuit of the machine into n sections, in which the flux density is approximately constant. Once the masses $m_{Fe,n}$ of the different n sections are calculated from the volumes and mass densities, the losses $P_{Fe,n}$ in these parts can be approximated as in (12). Here, $k_{Fe,n}$ are "loss" coefficients that, for a synchronous machine, can be imposed equal to 2 in teeth and to 1.6 in the yoke; $P_{10,f}$ is the loss density at 1 T and at the designed frequency of 200 Hz; $\widehat{B_n}$ is the maximum flux density in the n-th section (see Table II).

$$P_{\text{Fe}} = \sum_n k_{\text{Fe},n} P_{10} \left(\frac{\widehat{B_n}}{1T}\right)^2 m_{\text{Fe},n} \quad (12)$$

3) Mechanical and additional losses: a preliminary approximation of the mechanical losses can be also obtained using (13), where P_B and P_w are the friction and windage losses, respectively; k_m is an empirical coefficient from achieved from Reynolds constant for an Aluminium coolant

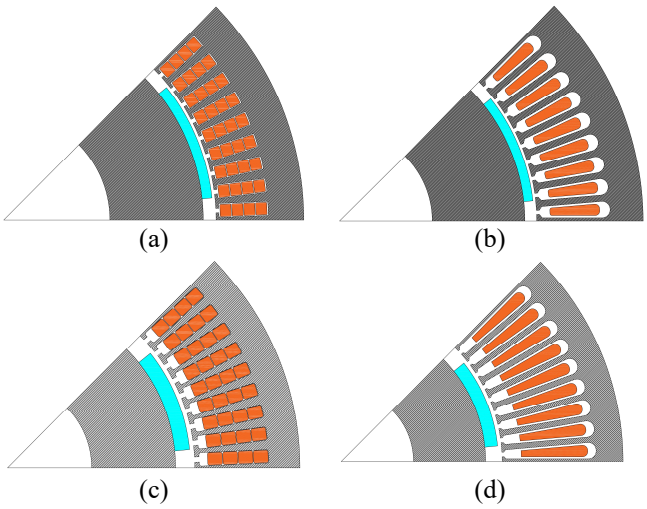

Figure 2 Machine geometries resulting from the preliminary analytical design with (a) hairpin windings at 200Hz; (b) round winding at 200Hz; (c) hairpin winding at 1000Hz; (d) round winding in 1000Hz

that is set equal to 2816 for 200 Hz and 5399 for 1 kHz; $m_{Fe,r}$ is the rotor mass. Measurement methods to determine the additional load losses P_{add} under sinusoidal supply conditions are given in the IEC 60034-2-1[19]. This loss value for a non-salient-pole synchronous machine is between 0.05 and 0.15 times the input power.

$$P_{mech} = P_B + P_w = k_m.m_{Fe,r}.n_m.10^{-6} + \\ +2D^3.{n_m}^3 L.10^{-14} \quad (13)$$

D. Design at increased frequency operation

To emphasize the high-frequency challenges of hairpin windings, the same design exercise described above is performed by selecting an operating frequency of 1000 Hz. To do so, a rated speed of 15000 rpm is initially assumed and the rated voltage value is increased up to 630V. Other quantities like flux densities, current density, expected output power and efficiency, materials, etc. are the same as the design carried out at 200 Hz. This design should result in a smaller motor with higher AC losses in the hairpin winding, thus eventually lowering the efficiency. It is expected that the constant factor of the reduced conductor height parameter (ξ) would be increased significantly in higher frequency for hairpin winding than the round one. Referring to (12), a higher value of $P_{10,f}$ is selected to take into account the frequency dependence of iron losses.

E. Summary of results

The geometries resulting from the preliminary analytical design process introduced above are illustrated in Figure 2, where random and hairpin winding machine designs at 200 Hz and 1000 Hz can be observed. A summary of the results obtained through the formulas introduced above is provided in Table IV for all the considered case studies. In general, smaller machine designs are achieved by increasing the operating frequency, for both random and hairpin windings. Consequently, volumes and masses are reduced at 1 kHz. Also, for a given frequency, the core size decreases from round to hairpin. This causes a reduction of iron losses by 24.6% at 200Hz and by 24.2% at 1000 Hz. Unlike the volume,

TABLE III SUMMARY OF THE ANALYTICAL DESIGNS FOR BOTH RANDOM AND HAIRPIN WINDINGS

F		200 Hz		1 kHz	
Main parameter	unit	Round winding	Hairpin winding	Round winding	Hairpin winding
l_m (PM thickness)	mm	3.36	3.36	3.36	3.36
D (outer rotor diameter)	mm	144.6	144.6	84.6	84.6
L (stack length)	mm	159.1	159.1	93	93
w_t (tooth width)	mm	2.3	2.3	1.4	1.4
w_y (stator yoke thickness)	mm	12	12	7	7
D_s (outer stator diameter)	mm	222.6	204.3	148.1	132
Stator core mass	kg	15.36	12.47	3.96	3.12
Rotor core mass	kg	20	20	4	4
Copper mass	kg	17.72	25.3	6.96	16.16
PM mass	kg	1.316	1.316	0.45	0.45
P_{Cu} (DC copper losses)	W	141	194	53	83.68
$P_{Cu,AC}$ (AC copper losses)	W	138	307	53	322.5
P_{Fe} (iron losses)	W	471.4	355.47	1809	1350
PM losses	W	19.3	13.92	15.6	12.88
P_{mech} (mechanical losses)	W	194	194	361.4	361.4
P_{ad} (additional losses)	W	47	47	47	47

it is irrefutable that with the choice of using a higher slot fill factor in the hairpin winding designs the mass density in round winding becomes higher than the hairpin one. The mass density in the round winding is more than hairpin one with 8.4% in 200 Hz and 28.8% in 1000 Hz. The higher fill factor used also results in higher DC copper loss in the hairpin winding. On the other hand, according to the hypotheses done above, the AC copper losses are considered only for hairpin conductors and as expected, these are much higher at high frequency. The next section aims to validate the analytical results through purposely built FE models of the machines and, most importantly, to provide a critical analysis on the limits of applicability of the analytical sizing tool for hairpin windings.

III. FE ANALYSIS – VALIDATION AND DISCUSSION

The geometries resulting from the preliminary sizing tool shown in Figure 2 are imported in the FE-based MagNet software for validation purposes and for carrying out in-depth critical analyses. A major difference in terms of modelling consists of using "stranded" and "solid" conductors for random and hairpin windings, respectively. This permits taking skin and proximity effects into accounts when the machines equipped with hairpins are analyzed. Also, when evaluating different frequency operations, the frequency of the current sources used to feed the three machine phases, as well as the speed imposed on the rotating components, are opportunely set. A suitable transposition in the hairpin winding models is used to avoid the presence of circulating currents among conductors [1].

A. Validation of analytical results

Before discussing the comparison between analytical and FE results in terms of global output quantities, such as those reported in Table III, the conditions in Table II for flux densities should be fulfilled. In Figure 3-6, the flux densities hypothesized for the analytical sizing (see Table II) are plotted as constant quantities in red, whereas the FE results are shown in blue as a function of the angular coordinate on a stator reference frame at a fixed rotor position. The three subplots of these figures report the flux density absolute values in the teeth, stator yoke and airgap of all the considered machines. In particular, the results for the motor with round windings at 200 Hz and 1000 Hz are shown in Figures 3 and 5 respectively, while those for the motor with hairpin windings at 200 Hz and 1000 Hz are shown in Figure 4 and 6. The match in any part of the studied machines is acceptable when the analytical findings are compared to the maximum flux density values obtained via FE analyses.

Regarding the output torque, Figure 7 plots the relevant trends for random and hairpin designs at 200 Hz obtained via the FE model, whereas Fig. 8 shows the same quantities but at 1000 Hz. These FE torque evaluations are relatively close to

TABLE IV COMPARISON BETWEEN ANALYTICAL AND FE RESULTS

	Frequency	**200 Hz**				**1 kHz**			
		Round winding		Hairpin winding		Round winding		Hairpin winding	
Main parameter	unit	Analytical Result	FEM Result	Analytical Result	FEM Result	Analytical Result	FEM Result	Analytical Result	FEM Result
P_{stator}(power losses of stator)	W	471.4	414	355.47	375	1809	1503	1350	1160
P_{cu}(DC copper loss)	W	141	170.9	194	193	53	60	83.68	83.78
k_{Ru}(R_{ac}/R_{dc})	-	1	1	1.6	4	1	1	3.9	10.7
Pcu,ac	W	138	170.9	307	763	53	60	322.5	892.8
Torque Mean value	N.m	120.85	117.5	122.7	113.5	23.78	23.48	23.7	22.134
Volume power density	MW/m3	6.25	5.69	7.4	6.88	23.3	22.7	29.2	27.9
Mass power density	W/kg	728.35	708.16	666.95	616.95	2503.24	2472.55	1781.38	1663.67
Volume torque density	KN.m/m^3	19.88	19.33	23.55	21.79	14.83	14.65	18.59	17.36
Mass torque density	N.m/kg	2.32	2.25	2.12	1.96	1.59	1.57	1.13	1.06
Efficiency	(%)	95.67%	93.02%	97.14%	89.85%	94.13%	92.97%	93.81%	87.61%
Output power	KW	37.97	36.91	38.55	35.66	37.35	36.90	37.23	34.77

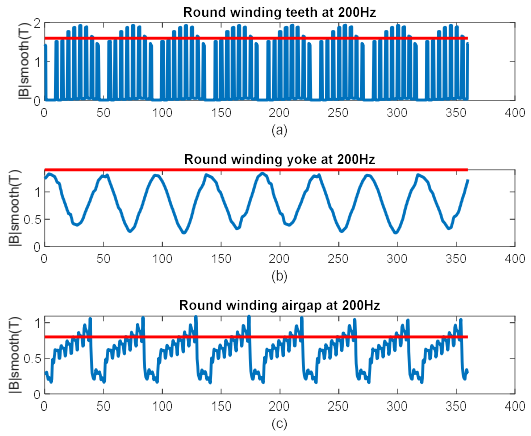

Figure 3 Comparison of analytical (in red) and FE (in blue) flux density values for the motor with round winding at 200 Hz in (a) teeth ,(b) yoke and (c) airgap

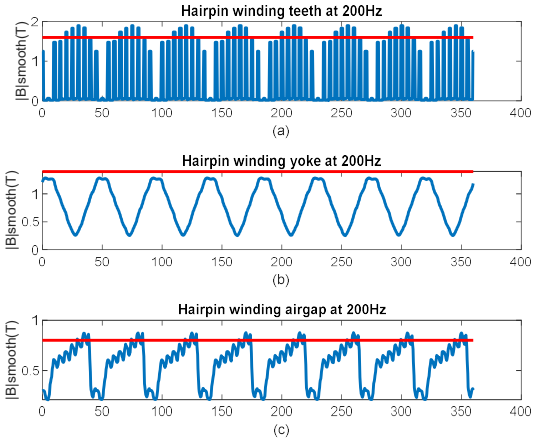

Figure 4 Comparison of analytical (in red) and FE (in blue) flux density values for the motor with hairpin winding at 200 Hz in (a) teeth ,(b) yoke and (c) airgap

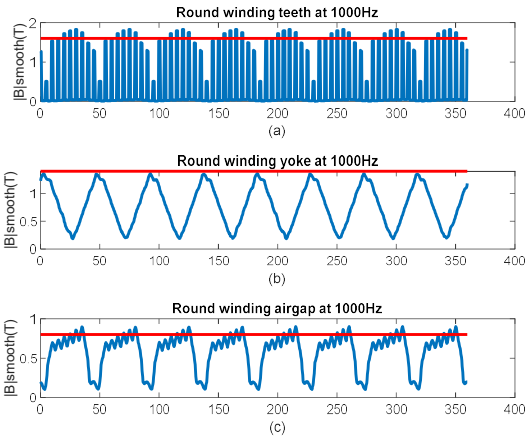

Figure 5 Comparison of analytical (in red) and FE (in blue) flux density values for the motor with round winding at 1000 Hz in (a) teeth ,(b) yoke and (c) airgap

the values assumed in the analytical calculations, with errors ranging from 2.3% to 7.22%. The exact average values are reported in Table IV, where also a comprehensive summary between the two methods for both random and hairpin designs is provided, at both 200 Hz and 1000 Hz. Most of the analytical values differ by 10% compared to FE results. However, the AC losses present the highest inaccuracy when comparing the two methods. For the hairpin design, the error

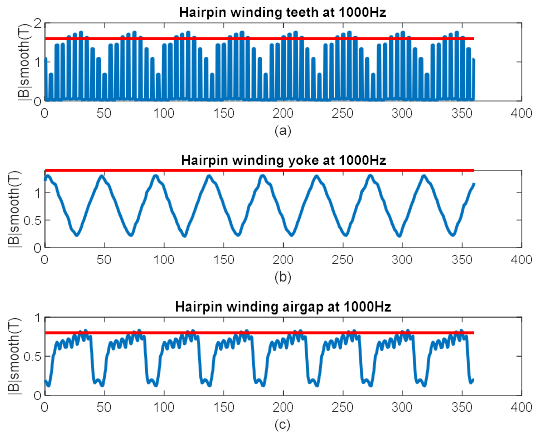

Figure 6 Comparison of analytical (in red) and FE (in blue) flux density values for the motor with round winding at 1000 Hz in (a) teeth ,(b) yoke and (c) airgap

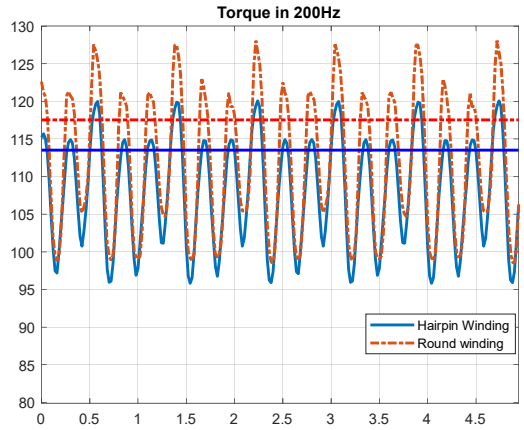

Figure 7 Output FE torque in hairpin and round winding designs at 200Hz

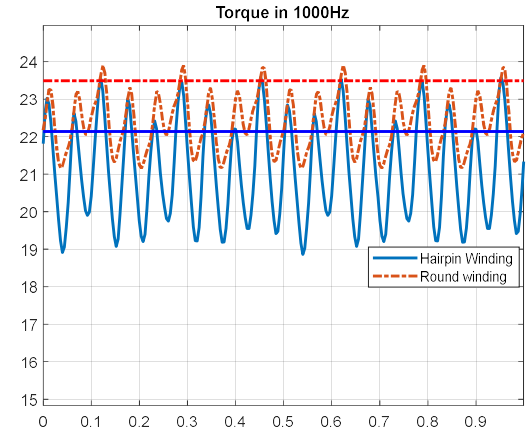

Figure 8 Output FE torque with hairpin and round winding designs at 1000Hz in FEM

for k_{Ru} is ≈60% at 200 Hz and ≈63.6% at 1000 Hz. Consequently, the comparison in terms of overall copper losses and efficiency is not accurate for hairpin windings, whereas for random windings is reasonable. In Table IV, power and torque densities for all the motors have been also compared for the sake of completeness.

B. *Further considerations and discussion*

Always for the sake of clarity and completeness, comparing the overall performance of random and hairpin winding designs, it can be concluded that at low frequency (200 Hz), the round winding design presents higher efficiency, mass torque and power density than the hairpin winding. This is due to the lower amount of copper used for the design of the latter. On the other hand, the hairpin winding designs have higher volume torque and power densities than the random winding ones at both the investigated frequencies.

Recalling that this work aims to prove the applicability of the classical preliminary sizing equations also for machines equipping hairpin technologies, it can be concluded that for an accurate estimation of AC copper losses and efficiency the analytical sizing tool cannot be used, regardless the frequency at which the machine is designed. On the other hand, this classical sizing approach can be used for accurately estimating quantities, such as the output torque and power, as it shows an acceptable accuracy (or at least similar to that achieved when the sizing equations are applied to the design of machines with random windings).

IV. CONCLUSION

In this paper, a comparative analysis was carried out between two surface-mounted permanent magnet synchronous machines for traction applications, one featuring a random-wound winding with round conductors and the other one equipping a hairpin winding. These two machine preliminary designs were performed at two different frequencies, i.e. 200 Hz and 1 kHz, to highlight the high-frequency challenges associated with hairpin conductors.

After the preliminary design process, carried out leveraging on the classical sizing equations for electrical machines, finite element models were built for validation purposes. The comparative analysis showed acceptable accuracy for most of the electromagnetic quantities of interest. However, when it came to AC losses and efficiency, the validity of the preliminary sizing tool highlighted significant limitations, although an AC losses prediction model was implemented for hairpin windings. Therefore, while for random-wound windings the classical sizing equations could be used with a certain level of “safety”, hairpin windings require more accurate and in-depth analyses and the relative sizing tools need to be improved.

ACKNOWLEDGEMENT

This project has received funding from the Clean Sky 2 Joint Undertaking under the European Union’s Horizon 2020 research and innovation programme under project AUTO-MEA grant agreement No. 865354.

REFERENCES

[1] Y. Zhao, D. Li, T. Pei and R. Qu, "Overview of the rectangular wire windings AC electrical machine," in CES Transactions on Electrical Machines and Systems, vol. 3, no. 2, pp. 160-169, June 2019.

[2] M. S. Islam, I. Husain, A. Ahmed and A. Sathyan, "Asymmetric Bar Winding for High-Speed Traction Electric Machines," in IEEE Transactions on Transportation Electrification, vol. 6, no. 1, pp. 3-15, March 2020.

[3] A. Hebala et al., "Feasibility Design Study of High-Performance, High-Power-Density Propulsion Motor for Middle-Range Electric Aircraft," 2020 IEEE 29th International Symposium on Industrial Electronics (ISIE), Delft, Netherlands, pp. 300-306, 2020.

[4] H. Park and M. Lim, "Design of High Power Density and High Efficiency Wound-Field Synchronous Motor for Electric Vehicle Traction," in IEEE Access, vol. 7, pp. 46677-46685, 2019.

[5] A. Arzillo et al., "Challenges and Future opportunities of Hairpin Technologies," 2020 IEEE 29th International Symposium on Industrial Electronics (ISIE), Delft, Netherlands, pp. 277-282, 2020.

[6] Hagedorn, Jürgen, Florian Sell-Le Blanc, and Jürgen Fleischer, Handbook of Coil Winding: Technologies for efficient electrical wound products and their automated production, Springer, 2017.

[7] F. Wirth, T. Kirgör, J. Hofmann and J. Fleischer, "FE-Based Simulation of Hairpin Shaping Processes for Traction Drives," 2018 8th International Electric Drives Production Conference (EDPC), Schweinfurt, Germany, pp. 1-5, 2018.

[8] Deming Zhu, Xin Qiu, Nan Zhou and Yangguang Yan, "A comparative study of winding factors between distributed windings and non-overlapping concentrated windings," 2008 Third International Conference on Electric Utility Deregulation and Restructuring and Power Technologies, Nanjing, pp. 2725-2729, 2008.

[9] M. Popescu, J. Goss, D. A. Staton, D. Hawkins, Y. C. Chong and A. Boglietti, "Electrical Vehicles—Practical Solutions for Power Traction Motor Systems," in IEEE Transactions on Industry Applications, vol. 54, no. 3, pp. 2751-2762, May-June 2018.

[10] T. Ishigami, Y. Tanaka and H. Homma, "Motor Stator With Thick Rectangular Wire Lap Winding for HEVs," in IEEE Transactions on Industry Applications, vol. 51, no. 4, pp. 2917-2923, July-Aug. 2015.

[11] F. Momen, K. Rahman and Y. Son, "Electrical Propulsion System Design of Chevrolet Bolt Battery Electric Vehicle," in IEEE Transactions on Industry Applications, vol. 55, no. 1, pp. 376-384, Jan.-Feb. 2019.

[12] G. Berardi and N. Bianchi, "High-Speed PM Generators for Organic Rankine Cycle Systems: Reduction of Eddy Current Rotor Losses," in IEEE Transactions on Industry Applications, vol. 55, no. 6, pp. 5800-5808, Nov.-Dec. 2019.

[13] G. Berardi and N. Bianchi, "Design Guideline of an AC Hairpin Winding," 2018 XIII International Conference on Electrical Machines (ICEM), Alexandroupoli, pp. 2444-2450, 2018.

[14] N. Bianchi and G. Berardi, "Analytical Approach to Design Hairpin Windings in High Performance Electric Vehicle Motors," 2018 IEEE Energy Conversion Congress and Exposition (ECCE), Portland, OR, pp. 4398-4405, 2018.

[15] A. Arzillo et al., "An Analytical Approach for the Design of Innovative Hairpin Winding Layouts," 2020 International Conference on Electrical Machines (ICEM), Gothenburg, pp. 1534-1539, 2020.

[16] D. B. Pinhal and D. Gerling, "Performance Map Calculation of a Salient-Pole Synchronous Motor with Hairpin Winding," 2019 IEEE 28th International Symposium on Industrial Electronics (ISIE), Vancouver, BC, Canada, pp. 359-365, 2019.

[17] M. Aoyama and J. Deng, "Visualization and quantitative evaluation of eddy current loss in bar-wound type permanent magnet synchronous motor for mild-hybrid vehicles," in CES Transactions on Electrical Machines and Systems, vol. 3, no. 3, pp. 269-278, Sept. 2019.

[18] J. T. J. a. V. H. Pyrhonen, Design of rotating electrical machines, John Wiley & Sons, 2013.

[19] 60034-2-1. IEC, "Rotating electrical machines - Part 2-1: Standard methods for determining losses and efficiency from tests". 27 06 2014.